

Influence of Laser Power on the Hardening of Ti6Al4V Low-Pressure Steam Turbine Blade Material for Enhancing Water Droplet Erosion Resistance

B.S. Mann, Vivek Arya, and B.K. Pant

(Submitted December 10, 2009; in revised form March 1, 2010)

To overcome water droplet erosion of Ti6Al4V alloy blade material used in low-pressure steam turbine (LPST) of high-rating nuclear and super critical thermal power plants, high-power diode laser (HPDL) surface treatment at two temperatures corresponding to two different power levels was carried out. During incubation as well as under prolonged erosion testing, the HPDL surface treatment of this alloy has enhanced its resistance significantly. This is due to the formation of fine-grained martensitic (α') phase due to rapid heating and cooling associated with laser treatment. The droplet erosion test results after HPDL surface treatment on this alloy, SEM, XRD analysis, and residual stresses developed due to HPDL surface treatment are given in this paper.

Keywords high-power diode laser, steam turbine, Ti6Al4V, titanium alloy, water droplet erosion

1. Introduction

Steam turbine moving blades used in low-pressure (LP) turbines are the critical components of a steam turbine. Stress corrosion cracking and wet steam erosion related failures account for one-third of total number of blade failures, especially in alloy steel blades and are the main causes of forced outages (Ref 1). On the other hand, excessive stresses generated due to centrifugal forces at the root of the alloy steel blades are critical, but these are less in titanium alloy because of lower density (4.42 g/cm^3). In addition to steady loads from rotation and steam flow, the blades are subjected to vibratory excitation as well. Under resonant conditions, the blade deflection and consequent stresses become so high that these blades may fail due to mechanical fatigue. It is essential to consider the fatigue behavior of blading alloy in impure steam condition (chloride and corrosive salt). These chlorides and corrosive salts cause excessive pitting of alloy steel blades (X20Cr13 and X10CrNiMoV1222). Available data show that the mean stresses of alloy steel blades are 275 MPa, and those of titanium alloy blades are around 170 MPa (Ref 1). When the wet steam becomes impure, the fatigue strength of alloy steel is affected significantly compared to that of titanium alloy. On the other hand to minimize power losses, a large exit annulus area of the steam turbine is needed. An increase in the last stage blade annulus area can be accomplished by using longer blades of lighter titanium alloy (Ref 2). In the above situation, the

titanium alloy (Ti6Al4V) becomes attractive as a LP steam turbine blading material. GE Toshiba has optimized this blade design based upon aerodynamic and mechanical considerations. For 1310 MW super critical steam turbine, Mitsubishi Heavy Industries Ltd has optimized new 74 inches moving blades for the last stage based upon titanium alloy. GE Toshiba is working on optimizing hybrid titanium as well as hybrid steel alloy blades. Due to their large size and high rpm (3600), the droplet erosion of these blades is a challenging problem, especially in nuclear turbines due to excessive wetness of steam that generally leads to early pitting and erosion. The water droplet erosion resistance of titanium alloy is rated inferior to the erosion resistance of conventional hardened alloy steel (flame, high frequency, or laser) and much inferior to stellite shielded 12% Cr steel. Stellite cannot be adopted for titanium alloy owing to expansion mismatch between these two alloys. It has been reported that high-power diode laser (HPDL) surface treatment has shown significant improvement in the droplet erosion; however, their erosion resistance is comparatively lesser than surface-treated X20Cr13 and X10CrNiMoV1222 alloy steel (Ref 3). More experimentation using different power of laser beam is required to obtain further improvement and better performance.

1.1 Conventional Heat treatment of Ti6Al4V Alloy

Pure titanium undergoes an allotropic transformation from the hexagonal close packed (HCP) alpha phase to the body centered cubic (BCC) beta phase at a temperature of $882.5 \text{ }^\circ\text{C}$. Alloying elements act to stabilize either the alpha or beta phase. Using alloying additions, the beta phase can be sufficiently stabilized to coexist with alpha at room temperature. This fact forms the basis for creation of titanium alloys that can be strengthened by heat treating. Rapid heat treatment of Ti6Al4V alloy becomes an important parameter that affects the mechanism and kinetics of phases and causes structural transformation. Information on refinement of grain structure, formation of microchemical homogeneity and substructure in

B.S. Mann, Vivek Arya, and B.K. Pant, Surface Coatings and Treatment Laboratory, BHEL, Corporate R&D Division, Vikasnagar, Hyderabad 500093, India. Contact e-mail: balbir@bhelmd.co.in.

the high-temperature phase following rapid heat treating has been addressed elsewhere (Ref 4). Ti6Al4V alloy has a low-thermal diffusivity ($0.03 \text{ cm}^2/\text{s}$) compared to that of alloy steel ($0.12 \text{ cm}^2/\text{s}$) and has a higher melting temperature ($1649 \text{ }^\circ\text{C}$) compared to that of alloy steel ($1500 \text{ }^\circ\text{C}$). Due to low-thermal diffusivity of Ti6Al4V alloy, the cooling rates during heat treatment play a vital role. Heating rates more than $100 \text{ }^\circ\text{C}/\text{s}$ followed by water quenching or forced air cooling give rise to fine grain structure, which improve the mechanical properties (high-yield strength $\sim 1100 \text{ MPa}$ and UTS $\sim 1226 \text{ MPa}$ along with good elongation $\sim 14.6\%$). By utilizing the concept of rapid heating and cooling associated with HPDL surface treatment, the best properties of this alloy are possible. Useful information, however limited, on water droplet erosion of laser surface melted Ti6Al4V alloy is available in the literature (Ref 5, 6). It has been reported that continuous wave CO_2 laser up to 5 kW in three discrete atmospheres, i.e., inert (pure Ar), Ar + $10\% \text{ N}_2$ and Ar + $20\% \text{ N}_2$ by volume was used for melting of titanium alloy at a set transverse speed of $20 \text{ mm}/\text{s}$ using an average laser power density of $5000 \text{ W}/(\text{cm}^2/\text{s})$. It has been reported that laser melting in an inert atmosphere resulted in homogeneous martensitic microstructure (α') to a depth of $400 \text{ }\mu\text{m}$ whereas in dilute nitrogen atmosphere, it has resulted in continuous TiN surface layer ($5\text{-}20 \text{ }\mu\text{m}$ thick) comprising of TiN plates, and it has also been reported that overlaps of 50% and 75% were maintained in Ar and Ar + N_2 environment, respectively. The average Knoop microhardness increased from 380 to $550 \text{ Kg}/\text{mm}^2$ at 50 g load. The water droplet erosion resistance of melted layer has improved $700\text{-}800\%$ while testing at $500 \text{ m}/\text{s}$ using $100 \text{ }\mu\text{m}$ water droplets (equivalent to impact energy of $65 \text{ }\mu\text{J}$).

In this study, the surface of Ti6Al4V alloy was not melted. It was heated close to the melting point of this alloy by limiting the HPDL power, its scan speed and controlling the heating and cooling rates. Details on the process adopted and experimental findings form the main part of this paper.

2. Experimental Procedure

2.1 HPDL Surface Treatment

Droplet erosion samples of size $12.7 \text{ mm } \varnothing \times 40 \text{ mm}$ length having internal threading M8 were made from Ti6Al4V material, typically used in LP end of high-rating steam turbines. A fixture was fabricated to hold and rotate these samples while carrying out HPDL surface treatment. Each sample was fixed in a self-centered three jaw chuck at one end and supported on a fixture on the other end. The fixture has a rotating seal, so that the samples can rotate freely and air used for cooling the samples does not leak. Rapid cooling of the sample was carried out during HPDL treatment by introducing compressed air having volumetric flow rate of $15\text{-}16 \text{ m}^3/\text{h}$ through the M8 tapped hole. This air is capable of removing heat at a rate of $160\text{-}180 \text{ W}$ which is comparable to the heat removed in a bulk titanium alloy during laser surface treatment. The samples were thoroughly cleaned using acetone before the start of the experiment to make the surface free from dust, oil, etc. The complete setup is shown in Fig. 1.

HPDL surface treatment was carried out on each sample using 4.6 kW Diode Laser System (Laserline GmbH). The laser head was mounted on a six plus two axis robot (Kuka GmbH).

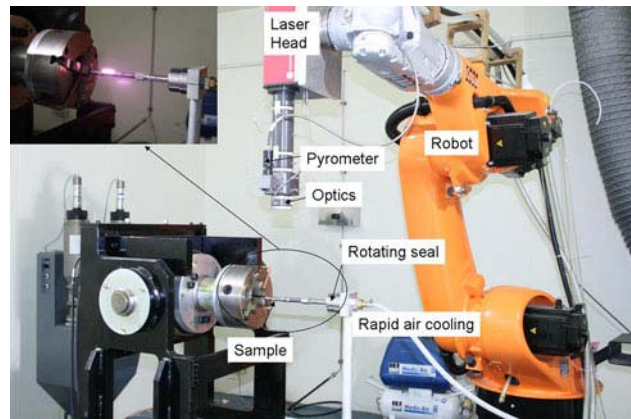


Fig. 1 Showing complete set up for doing HPDL surface treatment. (Inset: HPDL treatment being carried out on cylindrical sample)

Rectangular optics of “ $30 \text{ mm} \times 3.0 \text{ mm}$ ” and “ $20 \text{ mm} \times 2.8 \text{ mm}$ ” was used for the surface treatment of cylindrical and rectangular samples. Laser beam power was controlled in a closed loop by a two color pyrometer for achieving uniform surface temperatures. The complete system was controlled by the robot controller. The robot was programmed in such a way that the laser beam tracked the sample at a speed of $1.5\text{-}2 \text{ mm}/\text{s}$ ensuring that hardening of the sample was completed in one pass (lower speed for lower temperature). Thus, a wide area having a span of 30 mm on the outer periphery of the sample was laser hardened in one pass. The uniform compressed air cooling of the sample was maintained throughout the HPDL treatment process. The typical laser power used for the surface treatment of cylindrical samples was in the range of $735\text{-}870 \text{ W}$ resulting in maximum power density of $1635 \text{ W}/(\text{cm}^2/\text{s})$. These samples were stress relieved for 4 h after HPDL treatment and were then used for erosion testing.

2.2 Droplet Erosion Testing and Other Properties of HPDL-Treated Samples

2.2.1 Droplet Erosion Testing of HPDL-Treated Samples. The details of droplet erosion test facility are given in Ref 3 and 7. In short, the test facility consists of a 700 mm diameter chamber and a round stainless steel disc where the test samples are positioned. Samples, 40 mm in length and 12.7 mm in diameter are affixed on the periphery of the disc. The droplet erosion test details are given in Ref 3, and parameters are given in test II of Ref 3. Siemens have also carried out similar studies on X20Cr13 steel using $800 \text{ }\mu\text{m}$ droplets impinging at a velocity of $300 \text{ m}/\text{s}$ corresponding to an impact energy of 0.012 J . However, in this study, more accelerated conditions having droplet impact energy of the level of 0.38 J were adopted. This is to obtain the results in a short duration and to simulate the condition of a high-rating steam turbine corresponding to 74 inches long LP steam turbine blades where an impact energy level of 0.15 J occurs (based on $1/2 \text{ mV}^2$ for $800 \text{ }\mu\text{m}$ water droplet impacting at $\geq \text{Mach } 3$).

Cylindrical specimens were selected because the water impingement erosion occurs at the leading edge of actual steam turbine blades which are likely to have similar leading edge radii as those of the test samples. A precision balance ($\pm 0.1 \text{ mg}$) was used for measurement of mass loss after testing. The test duration depending upon energy and mass

fluxes was selected in such a way as to achieve steady-state erosion in limited cycles. The extent of erosion damage is calculated from the mass loss divided by the density of the material. The results have been plotted in the form of cumulative volume loss versus number of cycles.

The water analyses carried out in this study were as per Ref 3. The salt concentrations (calcium hardness ~110, magnesium hardness ~318, M-alkalinity ~228, P-alkalinity ~traces, chlorides ~146, sulfates ~52, and total solids ~854) were less than those reported in Ref 3. This has resulted in lower volume loss in droplet erosion testing compared to that reported in Ref 3.

2.2.2 Other Properties and Characteristics of HPDL-Treated Samples. The Vickers microhardness of HPDL-treated and untreated samples was measured by using Tukon 2100 Macro-/Microhardness tester (Wolpert, USA) by applying a load of 300 g with a dwell time of 13 s. The x-ray diffraction of HPDL surface-treated titanium alloy samples was taken using Philips X-pert system (Philips, the Netherlands). It was attempted to take residual stress measurements on HPDL-treated samples by using x-ray residual stress analyzer (Stress Tech, USA); however, this could not succeed. Round discs of size 80 dia. × 6 mm thickness were treated with HPDL by maintaining similar surface temperature and laser scan speed. Deflections arose in *X* and *Y* directions due to HPDL treatment, and these were physically measured. These deflections were used for the qualitative estimation of residual stresses.

3. Results and Discussion

3.1 Scanning Electron Micrographs

The scanning electron micrographs of droplet impingement eroded samples which were laser treated at two different temperature ranges after an operation of 5.13 million cycles are shown in Fig. 2-5. From the SEM of HPDL-treated samples, it is seen that the grain size is slightly smaller for the sample laser treated at higher temperature range 1700-1800 °C as compared to that treated at lower temperature range 1475-1625 °C.

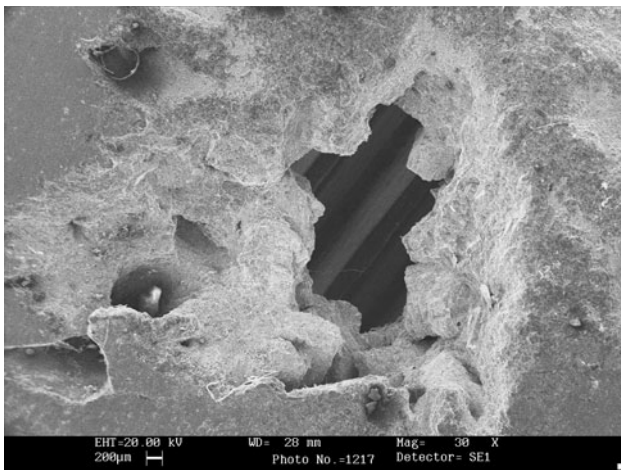


Fig. 2 After 5.13 million cycles, SEM micrograph of droplet impingement eroded HPDL-treated Ti6Al4V sample in the temperature range of 1475-1625 °C, showing extensive damage

However, there is a significant difference in their grain size to that of untreated Ti6Al4V alloy samples (Fig. 6). The material removal phenomena in the laser surface-treated samples appear to be grain by grain whereas in the untreated one it appears to be layer by layer. It is also mentioned in Ref 4 that fast heating and cooling rates produce fine microstructures and are responsible for improved mechanical properties (YS, UTS, and hardness) which are beneficial in enhancing the water droplet erosion resistance.

3.2 X-Ray Diffraction and Optical Microscope Findings

From the XRD, it is observed that the martensitic alpha phase has increased and beta phase has decreased after laser hardening compared to the untreated sample (Ref 3). It has also been reported that there is significant change in alpha peaks at two theta values at 35° and 40° and that of beta peaks at 2° values at 37.8° and 69.8° after laser hardening. XRD could not differentiate between α and α' phases except their peak counts.

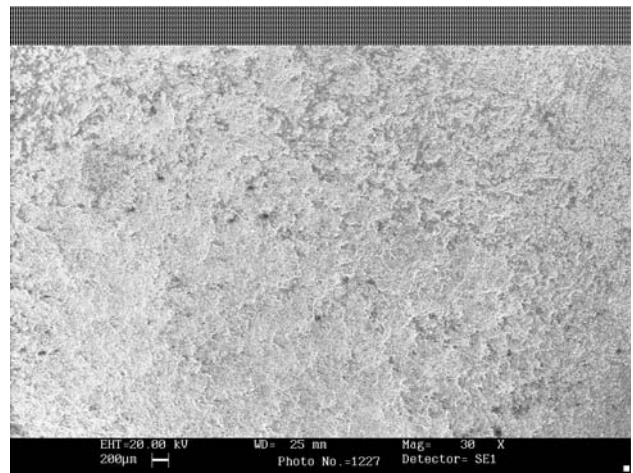


Fig. 3 After 5.13 million cycles, SEM micrograph of droplet impingement eroded HPDL-treated Ti6Al4V sample in the temperature range of 1700-1800 °C, showing very less damage

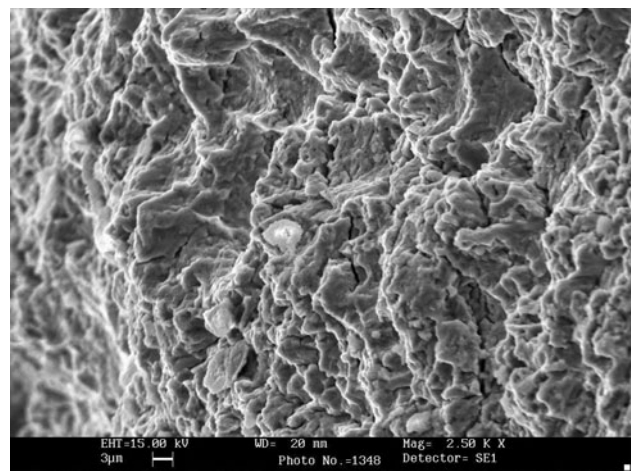


Fig. 4 After 5.13 million cycles, SEM micrograph of droplet impingement eroded Ti6Al4V sample HPDL-treated in the temperature range of 1475-1625 °C, showing material removal grain by grain

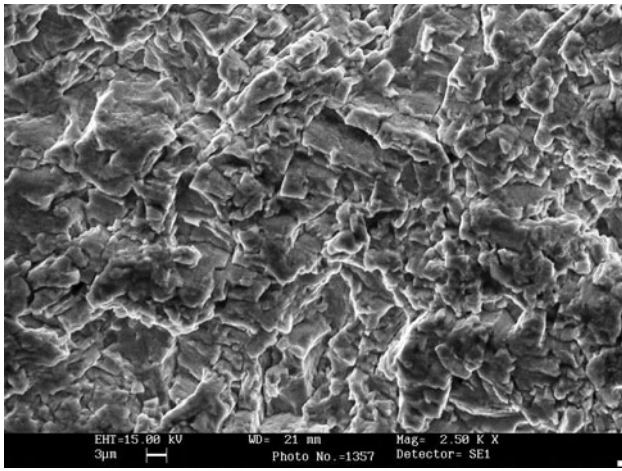


Fig. 5 After 5.13 million cycles, SEM micrograph of droplet impingement eroded Ti6Al4V sample HPDL-treated in the temperature range of 1700-1800 °C showing material removal grain by grain

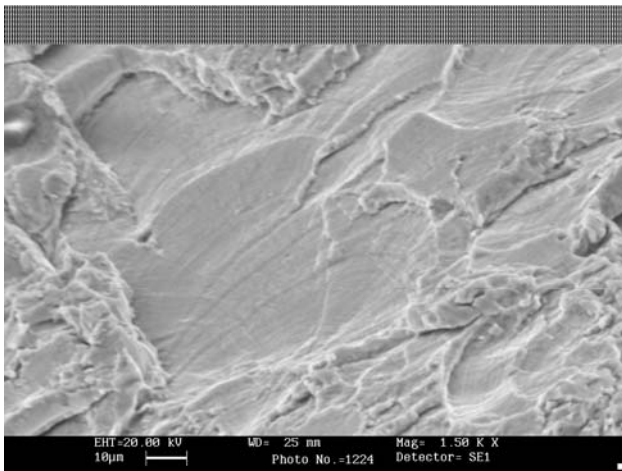


Fig. 6 After 2.28 million cycles, SEM micrograph of droplet impingement eroded untreated Ti6Al4V sample, showing material removal layer by layer

A significant change in alpha and beta peak counts for the sample treated at temperatures in the range of 1700-1800 °C compared to the sample treated at temperatures in the range of 1475-1625 °C is evident in their phases. Optical micrographs of untreated and HPDL-treated Ti6Al4V alloy samples were taken and their difference can be seen from micrographs given in Fig. 7 and 8. Some information on the microstructures of this alloy after diode laser treatment is available in Ref 8.

3.3 Residual Stress Measurement

For qualitative residual stress assessment, a round disc of size 80 mm dia. × 6 mm thickness was used. The round discs were chosen because the tips of the low-pressure steam turbine (LPST) blades have a curvature, though their radii may be different. The HPDL parameters such as the temperature of the sample, HPDL power, and laser scan speed were monitored and maintained similar to those of the cylindrical samples used for droplet erosion testing. The details of the deflections are given in Fig. 9. The deflections in round discs were measured using a

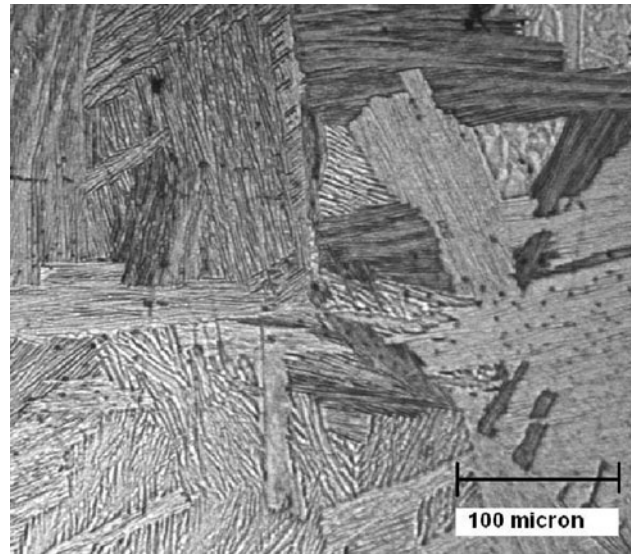


Fig. 7 Optical micrograph of untreated Ti6Al4V sample showing α and β structures

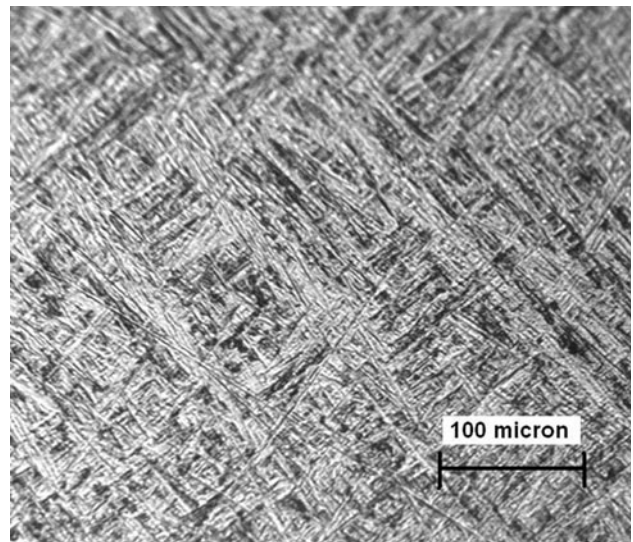


Fig. 8 Optical micrograph of Ti6Al4V sample HPDL-treated in the temperature range of 1700-1800 °C showing α and β structures

3D coordinate measurement machine. Maximum permanent bending was of the order of 520 μm in samples laser hardened at temperatures in the range of 1475-1625 °C and 540 μm in samples laser hardened at temperatures in the range of 1700-1800 °C in the Y direction. Maximum bending in X direction at both temperature ranges was 160 μm . This has resulted in proportionate compressive residual stresses in these directions. The radii of curvature arising due to deflections are given in Fig. 9. It is seen from Fig. 9 that the curvature is concave in both the directions and their magnitudes are different although these radii are similar to those reported in Ref 3. These result in compressive residual stresses in X and Y directions and their magnitude depend on their deflections. The deflection occurred in the X and Y directions are permanent in nature. This shows that the material has exceeded compressive yield strength value of 970 MPa (refer Ti6Al4V alloy material data sheet).

For Ti6Al4V LH 1550
 Laser Power: 920 W
 Power Density: 2300 W/(cm²/sec)
 Focal Length: 270 mm & Beam Size: 20x2.8 mm
 Laser Beam Travel: 2 mm/sec
 Max Deflection: 520 μm (Center of disc)
 Sample Size: 80Ø x 6 mm thick
 Surface treatment in the range of 1475 to 1625°C

For Ti6Al4V LH 1750
 Laser Power: 1035 W
 Power Density: 2587.5 W/(cm²/sec)
 Focal Length: 270 mm & Beam Size: 20x2.8 mm
 Laser Beam Travel: 2 mm/sec
 Max Deflection: 540 μm (Center of disc)
 Sample Size: 80Ø x 6 mm thick
 Surface treatment in the range of 1700 to 1800°C

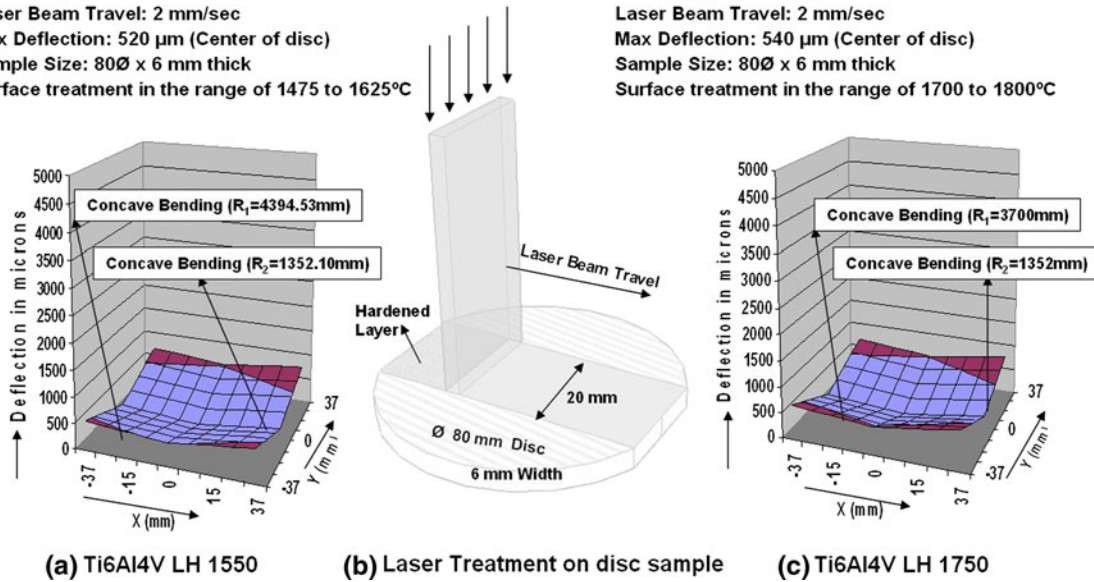


Fig. 9 Showing affect of Laser hardening temperature on the deflection occurring in Ti6Al4V disc

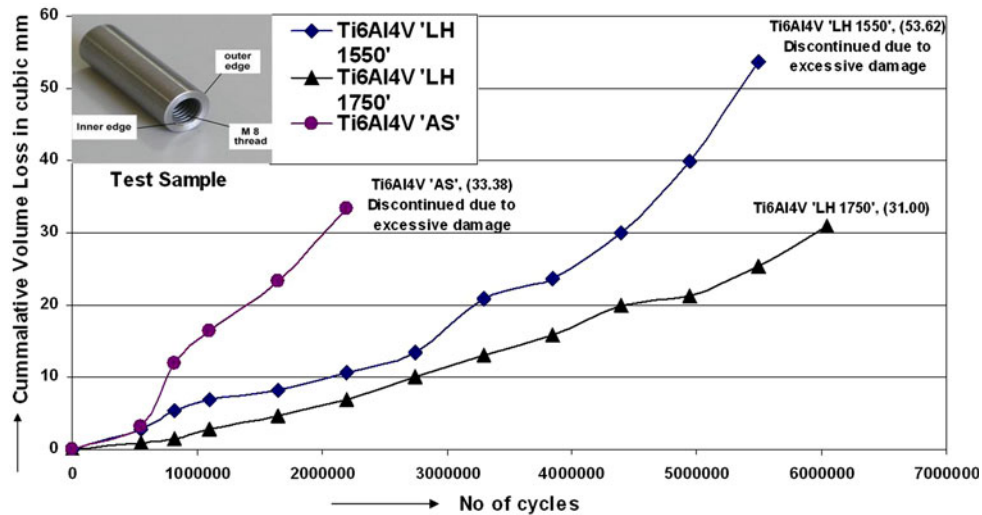


Fig. 10 Showing volume loss of Ti6Al4V alloy after HPDL hardening at droplet impact energy flux of 57.167 million J/m² s

The deflections and hence the stresses developed in a particular material depend upon the geometry of the sample, its thermal response, HPDL power, its scan speed, and direction. Information on flat rectangular samples of size 100 mm x 50 mm x 6 mm is available in Ref 3. For LPST moving blades, the value of these stresses may be different, but their trend of being compressive along and across the laser beam remains unchanged.

3.4 Droplet Erosion Test Results and Damage Mechanism

Information on the water droplet erosion damage mechanism of Ti6Al4V and steel alloys is available in Ref 9-11 and on

the microstructure and mechanical properties of Ti6Al4V alloy after various heat treatments is available in Ref 12. Actual damage measurements carried out on the LP steam turbine alloy steel blades for nuclear turbine are reported in Ref 10. In this study, the water droplet erosion resistance of HPDL surface-treated and untreated Ti6Al4V alloy samples was determined by mass loss measurements and these, based on volume loss, are plotted in Fig. 10. It can be seen from Fig. 10 that after an operation of 5.13 million cycles at an energy flux of 57.167 x 10⁶ J/m² s, maximum improvement has been observed for samples treated at temperatures in the range of 1700-1800 °C (two times improvement as compared to the sample treated at temperatures in the range of 1475-1625 °C).

Further improvement in droplet erosion with increased surface temperature was not observed. After laser treatment, the average hardness of the samples treated at above temperatures has increased to 365 HV at 300 g load from the base average microhardness of 316 HV. The untreated Ti6Al4V alloy sample suffered excessive damage after an operation of 2.28 million cycles and could not be tested further. The excellent droplet erosion resistance of laser treated Ti6Al4V alloy is due to improved mechanical properties and martensitic structure similar to that achieved in case of heat treatment to a temperature of 1050 °C followed by water quenching as reported in Ref 12. In this study, the high-cooling rates achieved are due to forceful extraction of heat by compressed air as shown in inset of Fig. 1 and also due to large cooling surface area of the cylindrical sample as shown in inset of Fig. 10.

4. Conclusions

The results of this study indicate that the laser surface-treated Ti6Al4V alloy has significantly improved the water droplet erosion resistance. This resistance has further improved with increased HPDL power by increasing the surface temperature of the samples in the range of 1700-1800 °C (two times improvement as compared to that in the range of 1475-1625 °C) and manifold improvement as compared to the untreated one. This is due to the formation of martensitic phase (α') similar to the martensitic phase formation in laser treated X20Cr13 steel.

Optical micrograph of the sample that has been HPDL-treated at temperatures in the range of 1700-1800 °C temperature has shown α' martensitic + β phase. XRD has confirmed increased alpha phase in this temperature range as compared to the sample treated at temperatures in the range of 1475-1625 °C. This increased alpha martensitic phase (α') appears to have an optimum balance of mechanical properties without compromising on ductility and resulted in enhanced droplet erosion resistance. The water droplet erosion resistance improvement is much more than the improvement reported earlier by melting of titanium alloy using higher laser power densities 5000 W/(cm²/s) compared to a maximum of 1635 W/(cm²/s) used in this study. Melting generally induces tensile residual stresses which are detrimental in droplet erosion.

Due to the limitations on the measurements of residual stresses in titanium alloy by conventional equipment, physical deflections after HPDL treatment of a round disc of size 80 dia. × 6 mm were measured. Maximum deflections permanent

in nature, of the order of 520 μ m in Y direction and 160 μ m in X direction at temperatures in the range of 1475-1625 °C, and 540 μ m in Y direction and 160 μ m in X direction at temperatures in the range of 1700-1800 °C were observed. These deflections have resulted in very high-compressive residual stresses in respective directions. These excessive compressive residual stresses are highly beneficial in improving the water droplet erosion resistance.

Acknowledgments

The authors are thankful to Mr. Venkateswar Reddy for doing Scanning Electron Microscopy and Dr. (Mrs) Y. Kalpana for providing information on water chemistry. The authors are also thankful to the management of BHEL Corporate R&D for permission to publish this paper.

References

1. R.C. Bates, J.W. Cunningham, and R.I. Jaffee, Corrosion Fatigue of Steam Turbine Blading Materials in Operational Environment, Final Report EPRI, CS 2932, 1984
2. A. Mujezinovic, Bigger Blades Cut Costs, *Modern Power Systems*, 2003, **23**(2), p 25–27
3. B.S. Mann, Vivek. Arya, B.K. Pant, and Manish. Agrawal, High Power Diode Laser Surface Treatment to Minimize Droplet Erosion of Low Pressure Steam Turbine Moving Blades, *J. Mater. Eng. Perform.*, 2009, **18**(7), p 990–998
4. O.M. Ivasishin and V.T. Roman, Potential of Rapid Heat Treatment of Titanium Alloys and Steels, *Mater. Sci. Eng. A*, 1999, **263**, p 142–154
5. C. Gerdes, A. Karimi, and H.W. Bieler, Water Droplet Erosion and Microstructure of Laser Nitrided Ti4Al4V, *Wear*, 1995, **186–187**, p 368–374
6. J.M. Robinson and R.C. Reed, Water Droplet Erosion of Laser Surface Treated Ti-6Al4V, *Wear*, 1995, **186–187**, p 360–367
7. B.S. Mann, V. Arya, and P. Joshi, Advanced HVOF Coating and Candidate Materials for Protecting LP Steam Turbine Blades against Droplet Erosion, *J. Mater. Eng. Perform.*, 2005, **14**(4), p 487–494
8. A. Lisieck and A. Klimpel, Diode Laser Surface Modification of Ti6Al4V alloy to Improve Erosion Wear Resistance, *Arch. Mater. Sci. Eng.*, 2008, **32**(1), p 5–12
9. A.S. Leyzerovich, *Wet Steam Turbine for Nuclear Power Plants*, Penwell Publication, 2005, p 169–170
10. B. Stanisa, Z. Schauperl, and K. Grilec, Erosion Behavior of Turbine Rotor Blades Installed in the Krsko Nuclear Power Plant, *Wear*, 2003, **254**, p 735–741
11. J.K. Reinker and P.B. Mason, Steam Turbines for Large Power Applications, GER-3646D, GE Power Generation Turbine Technology Reference Library, 1996
12. T.A. Venkatesh, B.P. Conner, C.S. Lee, A.E. Giannakopoulos, T.C. Lindley, and S. Suresh, An Experimental Investigation of Fretting Fatigue in Ti6AL4V; the Role of Contact Conditions and Microstructure, *Metall. Mater. Trans. A*, 2001, **32A**, p 1131–1146